Essential Readings in Light Metals: Aluminum Reduction Technology.
Edited by Geoff Bearne, Marc Dupuis and Gary Tarcy.

Light Metals — From ***Light Metals 2002***, Wolfgang A. Schneider, Editor

EFFECT OF THE BUBBLE GROWTH MECHANISM ON THE SPECTRUM OF VOLTAGE FLUCTUATIONS IN THE REDUCTION CELL

László I. Kiss, Sándor Poncsák

Université du Québec à Chicoutimi
555 boul. de l'Université Chicoutimi, Québec, G7H 2B1

Abstract

The spectrum of the voltage oscillations in the aluminum reduction cell depends on the size of the anode. Small laboratory cells and industrial size cells exhibit different fluctuation patterns. The growth of bubbles can be divided into two periods controlled by different physical mechanisms. The detachment frequency of the bubbles from the nucleation sites depends on the current density and detachment size, the latter being influenced by the material, microstructure and shape of the anode bottom. After detachment the main factor causing growth of the traveling bubbles is coalescence. A mathematical model that keeps track of each and every individual gas bubbles generated under the anode was developed and used to analyze the character of the fluctuations of the cell voltage. It is shown that in the case of industrial size anodes the voltage oscillations are dominated by the dynamics of the bubble interactions (coalescence) in the two-phase layer, while in small size laboratory systems the frequency of nucleation of the individual bubbles can be observed.

Introduction

Anode reaction produces carbon-oxyde gas bubbles during the aluminum electrolysis in the Hall-Héroult cells. The presence of an ensemble of bubbles under the anodes increases the bath resistance and the periodic generation, detachment and departure of the bubbles make the cell voltage fluctuate. Many researchers addressed the problem of gas bubble generation and voltage fluctuations in the past decades like (1,2,3,4,5), to cite only a few of them. Several factors motivate the efforts to improve the understanding of the spatial structure and temporal fluctuations of the gas bubble laden layer under the anodes: the reduction of cell resistance, quantitative description of the gas driven flow and the mass and energy transport inside the cell, better interpretation of the measured voltage oscillations etc.

Unfortunately, the direct observation of the two-phase layer in a real reduction cell is not feasible. Most of the published results in the field are based on laboratory experiments using room temperature hydrodynamic models (2) or laboratory size small electrolysis cells ("see-through cells") (3,5).

The character of the voltage fluctuations in an electrolysis cell is complex, but certain regular features can be discovered even without a deep quantitative analysis. This is especially true in small, laboratory sized cells, where only a few bubbles exist simultaneously under the anode. Most researchers agree that under such circumstances the high frequency, low amplitude component of the spectrum is associated with the periodic nucleation of the individual bubbles, while the slower, high amplitude oscillations are caused by the departure of the big, coalesced bubbles from the side edge of the anode.

The generation of the gas under the anode has a discrete, repetitive character both in space and time. First, the bubbles are generated at certain preferential points, in the so-called nucleation sites (10) that form a geometric array or mesh along the bottom surface of the anode. As the current density is nearly uniform along the anode surface and the properties of the anodes do not vary significantly in space, one can assume that the distance between neighbouring nucleation sites - or the number of sites per unit surface - does not show a great variation. Second, the nucleation of gas bubbles in the electrolyte has a periodic character – similarly to that in boiling – as the continuous growth following the nucleation is interrupted when the so-called detachment condition is achieved. The detachment or release of the individual bubbles from their respective nucleation sites breaks the process into short, more or less uniform growth cycles.

It seems plausible for the first sight that the above outlined discrete spatial and temporal structure of bubble generation plays a basic role in shaping the voltage fluctuations. However, there are other discrete events besides the nucleation and detachment of the individual bubbles that exert a strong influence on the dynamics and structure of the two-phase layer under the anode. After the detachment, the growth of the bubbles is mainly controlled by coalescence, which leaves strong and distinctive marks on the voltage fluctuations.

In order to improve the understanding of the underlying mechanisms that control the frequency of nucleation of individual bubbles, an analysis of different scenarios was completed earlier (7). That study concluded that in the case of porous carbon anodes, the nucleation cycle is controlled by the storage and diffusion of the gas in a thin layer along the anode bottom. In a second part of that research an ensemble of nucleation sites were modeled and the structure of the whole bubble layer was described in its evolution (8). The mathematical modeling of the bubble layer supplies – among other parameters – the fluctuations of the covering factor and that of the mean velocity of the gas bubble laden layer.

The objective of the present paper is to analyse the effect of the factors controlling the growth of the bubbles on the spectrum of the voltage fluctuations by using the mathematical simulation as a tool.

Growth of individual bubbles

As it was mentioned above, the bubbles are generated at the nucleation sites periodically. A complete growth cycle starts with a latent period. In the latent period the gas produced by the electrolysis is picked-up and stored by absorption-adsorption on the surface of the anode, building up the necessary pressure to start to inflate a bubble. From that point, the bubble grows continuously to the detachment, when the buoyancy and hydrodynamic forces – exerted on it by the moving liquid – become equal to the surface forces tying the bubble to the anode. After detachment a new cycle starts. The gas (CO_2) is continuously generated along the electrolyte-anode interface where carbon, oxygen and electrons are all available. There is no gas generation along the surface of the bubble (gas-liquid and gas-solid interfaces); consequently a transport and storage mechanism between the place of generation and the bubbles must exist.

Three potential mechanisms for the gas storage and transfer were examined:

a) The gas is dissolved in the bath and is transferred to the bubble by diffusion in the liquid phase.
b) The gas is stored in the pores of the anode and migrates to the bubble through the pores.
c) The gas is captured on the surface of the anode by adsorption and is transferred to the bubble along the perimeter of solid-gas contact zone by desorption.

Mechanism a) provides a good explanation for bubble growth in aqueous electrolytes, as water can easily dissolve large quantities of gas. Our earlier analysis (7) has shown that in aluminium electrolysis scenario a) cannot explain the rate of bubble growth especially due to the very low diffusivity and solubility of the CO_2 gas in the molten electrolyte. The adsorption-desorption mechanism seems to give an adequate explanation in the case of non-porous (for example glassy) anodes. On the other hand, the porosity of the presently used industrial carbon anodes offers sufficient storage and diffusion capacity in a thin (1-3 millimetre thick) adjacent layer along the bath-solid interface to explain measured bubble generation frequencies by the second scenario above (7). This is supported by the observation that the electrolyte does not penetrate into the pores of anodes during normal operation, but it happens after the current was shut. It must be noted that the adsorption of gas on the internal surface of the pores can also be present in this case, so the gas can be stored by a combination of volume and surface effects inside the pores.

The volume of the bubbles when they detach from the nucleation site has a strong influence both on the frequency of bubble generation and on the number of the active nucleation sites on the anode surface. In spite of its importance in controlling the spatial and temporal structure of the bubble layer, the physics of the bubble detachment is not fully understood. Kloucek and Romerio (9) analyzed the free energy of the bubble during its growth and they explain the detachment of a bubble as a first order phase transition. Their explanation gives an upper limit on the size of a bubble under static, equilibrium conditions. A bubble bigger than the critical size will be separated from the solid by a liquid film even when there is no any liquid movement present.

In (7) the detachment size is calculated from a dynamic condition, using a force balance equation between the drag force and surface forces. The drag force on the bubble is increasing with its volume faster than the resistance due to its deformation to the point when the drag overcomes the retaining force and the moving two-phase layer entrains the bubble. Based on some empirically obtained bubble deformation data, the calculations show that the bubble has about 5-6 mm horizontal diameter and 2.5-3 mm height at detachment.

Bubble frequency, number of nucleation sites

As the bubbles are repetitively generated in discrete points, there is a small gas producing area around the nucleation centres that feeds the growing bubble with gas. A nucleation centre with this associated area can be called an "elementary cell". The size of this elementary gas-producing surface is linked to the frequency and detachment size of the bubble and to the operational parameters of the cell through the Faraday equation:

$$n \cdot z \cdot F = \frac{P \cdot V}{R_u \cdot T} z \cdot F = i \cdot A \cdot t \quad (1)$$

where n is the number of moles of the gas, z is the number of charges involved in the electrochemical reaction, F is the Faraday constant, P and V are the pressure and the volume of the gas evolved during the time t, R_u is the universal gas constant, T is the temperature, i is the nominal current density, and A is the total bottom surface of the anode.

If the detachment volume of one bubble is V_b, then the total number of bubbles generated under the whole anode in unit time is $N_b = V/(V_b \cdot t)$. Furthermore, if the area of an elementary gas generating cell is A_0, then the number of active nucleation sites along the anode surface will be $k = A/A_0$. With these notations the frequency of bubble generation at a single nucleation site is

$$f = \frac{N_b}{k} = \left(\frac{iR_uT}{PzF}\right)\left(\frac{A_0}{V_b}\right) \quad (2)$$

The first group on the right side of the equation includes the operational parameters of the cell like the current density, temperature, bath level (pressure), while the second group characterizes the size of the space domain where the individual bubbles are generated. The minimal value of the A_0 elementary gas-generating surface is limited by the detachment size, as it must be bigger than the contact area of the bubble in the instant of detachment (otherwise the growth of the bubble would stop before the detachment size achieved). The maximal size of A_0 depends on the gas storage capacity and on the resistance to the gas transport process as well as on the type of coupling between nucleation sites and elementary cells. In principle an elementary gas-generating surface can feed one or more nucleation sites. In the first case all the nucleation sites must work simultaneously – or at least nearly simultaneously. In a more complex pattern, bubbles are generated alternatively at neighbouring nucleation sites and the elementary gas generating cells overlap.

Growth rate of individual bubbles

The growth of individual bubbles has a smooth and continuous character before the detachment, except the relatively short initial latent period. The growth of the bubbles is controlled by diffusion. When the gas is stored in the electrolyte (aqueous systems) the volume-time history can be described analytically by a 3/2 power law, figure 1.

The character of the bubble growth in an aluminium reduction cell where the storage and transport of gas takes place in the porous anode is also shown in Figure 1, as it was obtained by numerical simulation (7). For an easier comparison of their shapes, the two curves were normalized with the duration of the growth cycle and with the detachment volume. As the computed curve (b) in figure 1 shows, the growth rate is increasing as the bubbles become bigger. The growth curve was computed by using a forward marching (evolving) time scheme, which determines in each time step

- the current density that is decreasing as bubble grows,
- the gas generation on the liquid-solid interface,
- the distribution of the gas concentration inside the anode by solving the diffusion equation,
- the mass transfer rate through the bubble-solid interface,
- the new volume and shape of the bubble,
- the balance between drag and retaining forces to decide whether the detachment condition was achieved.

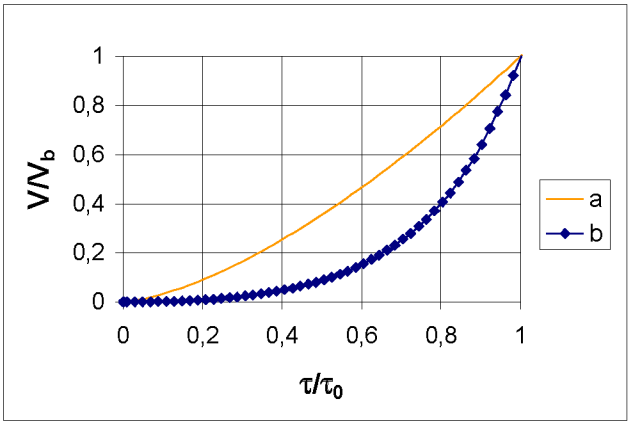

Figure 1. Normalized bubble growth curves. Growth is controlled by diffusion in the liquid (a) and by diffusion in the porous anode (b).

During the diffusion-controlled growth, the increase of the diameter of the bubbles covers 2-3 orders of magnitude from a few micrometers to about half centimeter. Correspondingly, the bubble volume increases several million times during this period. The t_0 period of the diffusion controlled growth is estimated to be somewhere between 100 and 400 milliseconds depending on the design and operating conditions of the cell.

Coalescence-controlled growth

After detachment, the bubbles are surrounded completely by the electrolyte in which the diffusion of the gas toward the bubble is practically negligible. The only way left for the bubbles is to grow by coalescence. After detachment, the bubbles are swept away by the liquid-gas layer moving horizontally under the anode. During their voyage they collide and eventually coalesce. Different sized bubbles follow the overall flow with different relative velocities. The velocity differences and the bigger diameters increase the probability of coalescence thus the rate of growth increases during this period too.

A mathematical model was developed earlier to simulate the structure and dynamics of the bubble-laden layer under the anode in an aluminium electrolysis cell (8).

In the model there is a one-to-one correspondence between the nucleation sites and elementary gas-generating surfaces, e.g. a surface element feeds always the same nucleation center. An important issue that influences the temporal character of simulated voltage fluctuations is how the individual nucleation centers are arranged along the anode surface and how they are triggered. If the bubbles are generated in the nodes of a regular, uniformly spaced mesh and all of them start the nucleation cycle at the same instant, the fluctuations of the gas covered portion of the anode will be very much regular, including a few harmonic oscillations. In the reality, although the structure of the anodes is homogeneous on the centimeter scale ("mesoscale"), below that scale, on the millimeter and micrometer level ("microscale") there are big

variations in the properties of grains and pores. To reflect the effect of the real anode structure in the model, the mesoscale homogeneity was respected by tiling the anode surface with uniform elementary gas generating cells. Although square elements were also considered preliminarily, the hexagonal elements shown in Figure 2 were chosen for the vast majority of the simulations. As in the real world the nucleation centers are not aligned along straight lines like the dotted lines in figure 2, the nucleation centers were randomly placed inside a circle around the nodes of the mesh. The diameter of the circle inside the elementary cell characterizes the scale of inhomogeneity in the anode. The diameter of the circle was chosen to respect a certain minimal distance between the neighboring nucleation centers.

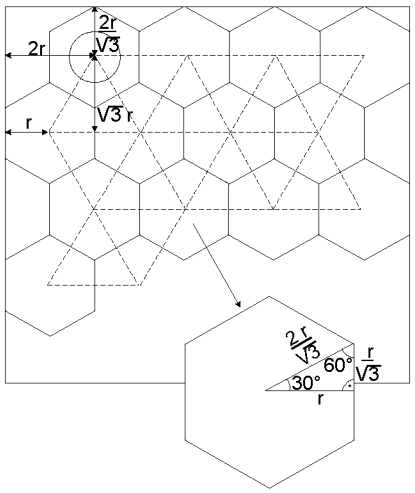

Figure 2. Mesh of nucleation centers along the anode surface.

There is no physical mechanism that would trigger the nucleation of the bubbles at the same instant everywhere on the anode. The pore size distribution and the random character of surface roughness create nucleation sites where the pressure necessary to initiate bubble growth varies randomly between certain limits. The beginning of the bubble cycles is not synchronous, the random distribution of the grain and pore sizes necessarily introduce a certain randomness into the beginning of the nucleation at various sites. On the other hand, the conservation of charge and mass require that the bubbles remove the total gas generated by the electrolysis within a given period of time. Small fluctuations can occur due to storage effects (cyclic filling and emptying of the pores, or adsorption-desorption), but on a longer scale the volumes of gas produced and released must be equal. Our simulation respects the conservation principles by introducing temporal randomness only within a time scale equal to the period of the nucleation cycle.

The algorithm keeps track of all the bubbles generated at the nucleation sites from their "birth" through their travel under the anode and their rise in the side channel to the point when they escape on the upper horizontal surface of the bath. Results presented in this paper were all computed for 280 elementary cells. This number of sites allows studying the bubble layer below anodes of up to about 320-millimeter length. It must be noted that the number of bubbles that exist simultaneously under the anode is about two times bigger than the number of the nucleation sites.

The step-by-step algorithm

- controls the triggering of the nucleation cycles in the elementary cells,
- checks the detachment condition,
- calculates the size of the bubbles while they are in the diffusion controlled growth,
- checks the condition of coalescence for moving and stationary bubbles,
- calculates new size and position of the coalesced bubbles
- calculates and stores the size, position and velocity of each and every bubbles under and beside the anode,
- calculates the actual volume fraction of the gas under the anode and in the vertical side channel,
- determines the covering factor (or simply the covering) of the anode,
- determines the mean velocity of the bubble laden layer using the momentum equation.

The primary, raw results of the simulation are the arrays containing the position, diameter, volume and velocity data for the thousands of bubbles in the two-phase layer. By using these data, the collective influence of the bubbles on the covering factor and bubble layer velocity can be determined. Another computational module was developed to visualize the dynamically changing structure of the bubble-laden layer as a video film.

The most comprehensive results of the simulation are the calculated fluctuations of the covering factor and that of the velocity of the bubble-laden layer. They reflect well the character of the voltage fluctuations found experimentally in different sized electrolysis cells (5,6).

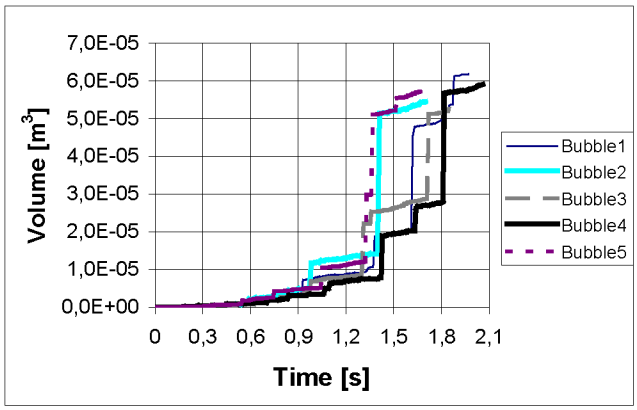

Figure 3 Coalescence controlled growth of five different bubbles – numerically simulated scenario.

The character of the growth of bubbles after the detachment, in the coalescence-controlled period is illustrated in Figure 3. The law of growth is non-continuous; each sudden increase in bubble volume corresponds to a coalescence event. Furthermore, the growth curves are not identical. This is a result of the random deviations from the perfectly regular spatial and temporal distribution of the nucleation centers, built into the model as described above. In the coalescence controlled period, the horizontal diameter of the big bubbles increases about 20 times - depending on the anode size – but the volume of them gets bigger only about 500 times due to their flattened shape. After

detachment the volume of the bubbles increases mostly by spreading horizontally, the vertical dimension of the bubbles is practically constant.

Results and Discussion

All the simulations presented below were made for the case of a perfectly flat and horizontal, porous anode. The model has the potential to simulate real-shaped (curved) anode bottoms, grooved and non-porous anodes. These computations are presently under way, the results will be reported later.

The above outlined simulation tool was used to analyze the influence of the anode size and that of the growth mechanism on the voltage fluctuations. First the effect of the length of travel below the anode is presented in Figure 4.

The numbers in the figure indicate how many elementary cells are placed on the anode surface. The first and second values stand for the number of elementary cells along the parallel (length) and perpendicular (width) directions to the flow, respectively.

Effect of anode length

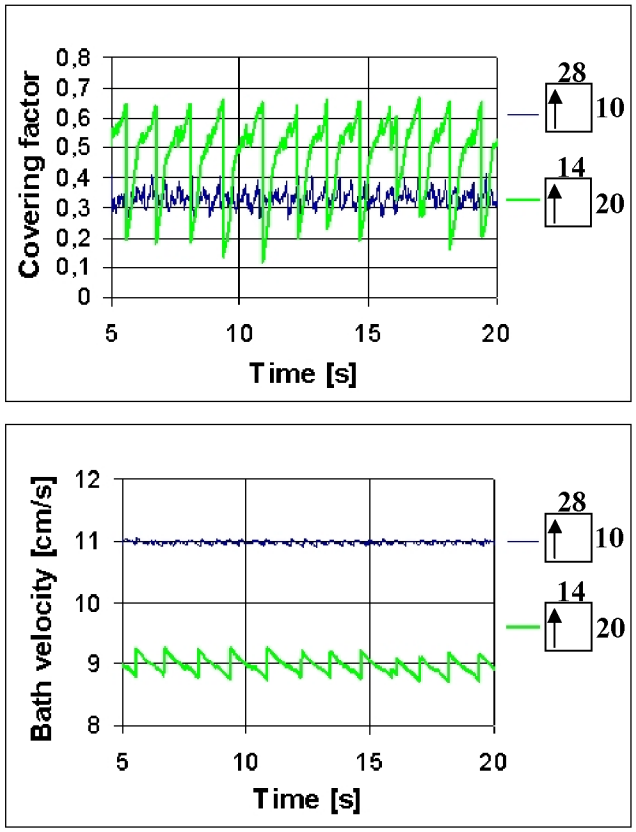

Figure 4. Influence of the length of the anode on the voltage and velocity fluctuations

With increasing length-to-width ratio both the mean value and the amplitude of the voltage (covering factor) fluctuations get bigger. This can be explained by the increased chance for the bubbles to coalescence during their travel. The large gas pockets dominate the behavior of the gas-laden layer by sweeping the whole anode surface before they escape at the anode edge. At the moment of release, the gas covered portion of the anode decreases sharply. When the big bubbles enter the side-channel, their rise to the free surface accelerates the whole bubble-layer suddenly, as it can be seen in the lower part of Figure 4. The amplitude of the velocity fluctuations is much bigger than in the case of shorter anodes. On the other hand, the average value of the velocity is lower in this case, as the longer travel of the big gas pockets create more retaining force than the shorter path of the ensemble of smaller bubbles.

To have a deeper insight into the phenomena, the spectrum of the simulated voltage fluctuations was determined by Fourier analysis. The results for the two geometries are shown in Figure 5. In the case of the shorter anode (10x28), there are two strong, distinctive peaks in the spectrum within the 2-10 Hz range. The doubling of the length of the anodes (20x14) permits the bubbles to organize themselves into bigger gas pockets that are released at a lower rate, less than 1 Hz. The higher harmonics are effectively suppressed, but the maximum amplitudes become about 4 times bigger than in the case of shorter travel.

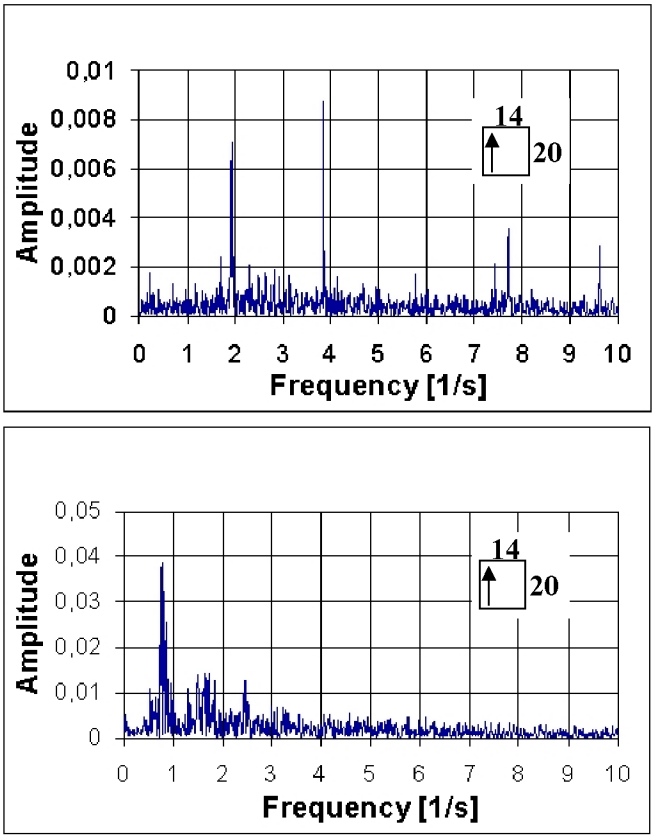

Figure 5. Spectrum of the voltage fluctuations for different anode lengths

Effect of the growth law in the diffusion-controlled period

Secondly the effect of changing the growth law was analyzed. The growth law computed for the case of gas storage and diffusion in the porous anode (curve **B** in Figure 6) was compared with an arbitrarily chosen, linear law (line **A**).

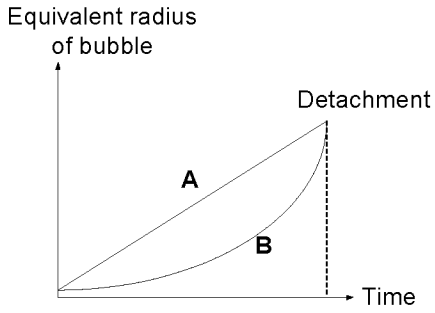

Figure 6 Growth laws: A linear, B diffusion controlled

The simulated voltage and velocity fluctuations for the two different growth laws are shown below in Figure 7, for the 20x14 anode geometry. It can be concluded that while the factors like detachment size, bubble release frequency, distribution of nucleation centers are kept identical, the actual shape of the growth curve before the detachment does not play a decisive role in forming the voltage fluctuation of the whole cell.

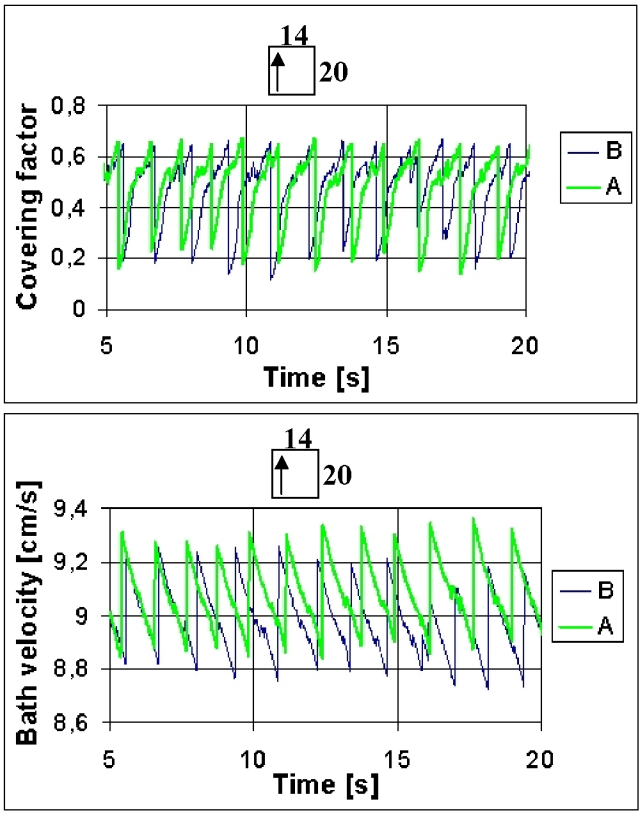

Figure 7 Effect of the growth-law on the voltage and velocity fluctuations

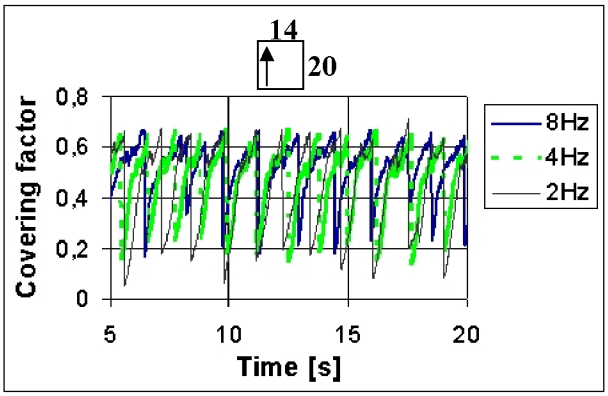

Figure 8. Voltage fluctuations at different detachment frequencies.

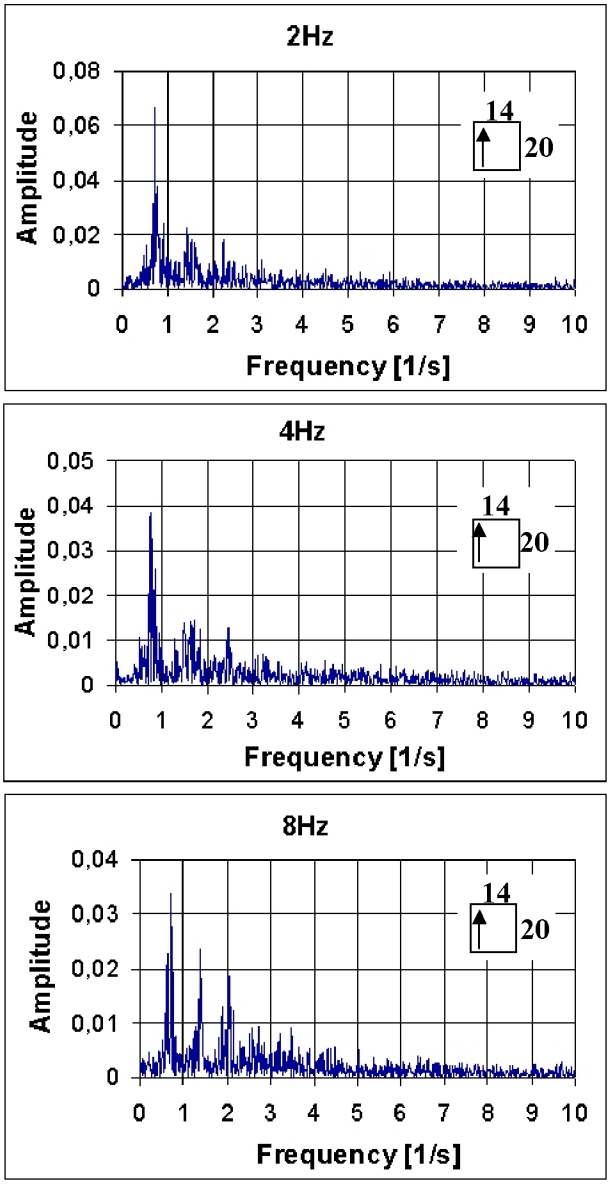

Figure 9. Spectrum of the voltage fluctuations at different detachment frequencies

Although the relative increase of the bubble size in the diffusion controlled, first period of growth is much bigger than the rate of increase in the second, coalescence period, the second period dominates the overall picture. This effect will be further illustrated below by the analysis of the influence of the bubble detachment frequency on the voltage fluctuations.

Influence of the detachment frequency

To show the weak effect of the behaviour of the individual bubbles - sitting and growing at the nucleation sites - on the entire bubble layer, the impact of different bubble formation frequencies (2, 4 and 8Hz) on the voltage spectrum was examined. In order to respect the mass balance, the detachment volume of the bubbles was also modified to $1.6 \cdot 10^{-7}$, $8 \cdot 10^{-8}$, $4 \cdot 10^{-8}$ m^3 according to the various frequencies.

The graphs of the voltage fluctuations (
Figure 8) as well as the spectra in Figure 9 do not show a fundamental difference as the frequency of detachment varies between 2 and 8 Hz. The dependence of the maximal amplitude of the fluctuations on the detachment frequency is visible, but the mean value of the covering factor and the characteristic frequencies vary only slightly.

The most interesting feature of this comparison is that there is no any visible peak in the spectrum at the detachment frequency. Consequently, it is very difficult to extract the frequency of the nucleation of the individual bubbles from the voltage fluctuations measured on a large, industrial cell. In these cells, the interactions among the moving bubbles, their coalescence and release at the edge of the anode dominate the spectrum of the voltage fluctuations.

Conclusions

Using a previously developed mathematical model the influence of different parameters of the bubble growth on the voltage fluctuations in the Hall-Héroult cell was analyzed by simulation.

It was found – in accordance with the experiments and practical observations – that the events during the coalescence-controlled period of bubble growth dominate the spectrum of the fluctuations.

The length of the anode exerts a strong influence on the voltage fluctuations. The longer travel of the bubbles under the anode gives more chance to coalescence, the bubbles grow bigger that finally results in bigger amplitude of fluctuations at a lower characteristic frequency.

On the other hand, the details of the nucleation of the bubbles - like the form of the law of growth before detachment and the frequency of detachment - are overshadowed by the dominant effects during the coalescence-controlled period.

Acknowledgements

The present work was supported in part by an NSERC-ALCAN research grant. One of the authors (SP) gratefully acknowledges the support provided by a Graduate Studies Scholarship from the Ministry of Education of Quebec.

References

1. O.A. Asbjørnsen, J.A. Andersen, A. Larsen, "On the use of mathematical models for the physical interpretation of current and voltage fluctuations in an alumina reduction cell", TMS Light Metals, 1979, 517-539.
2. S. Fortin, M. Gerhardt, A.J. Gesing, "Physical modelling of bubble behaviour and gas release from alumium reduction cell anodes", TMS Light Metals 1984, 721-741.
3. J. Xue and H. A. Øye, TMS Light Metals, 1995, 265-271.
4. N. E. Richards, "The dynamics of components of the anodic overvoltage in the alumina reduction cell," TMS Light Metals, 1998, 521-529, (1998).
5. X. Wang and A. T. Tabereaux, TMS Light Metals, 2000, 239-248.
6. T. M. Hyde and B. J. Welch, "The gas under anodes in aluminium smelting cells, Part II. Measuring and modelling bubble resistance under horizontally oriented electrodes", TMS Light Metals, 1997, 333-340.
7. S. Poncsák, L. I. Kiss, R. T. Bui, "Mathematical modelling of the growth of gas bubbles under the anode in the aluminium electrolysis cells", CIM Light Metals, 1999, 57-72.
8. S. Poncsák, L. I. Kiss, R. T. Bui, P. Desclaux, J-P. Huni, V. Potocnik, "Mathematical modelling of the collective behaviour of gas bubbles under the anode", CIM Light Metals, 2000, 139-154.
9. P. Klou□ek, M. Romerio, "The first order phase transition of bubbles at solid-liquid interfaces", EPFL Lausanne, No. 01.2001, January 2001.
10. J. E. Sgheiza and J. E. Myers, "Behaviour of nucleation sites in pool boiling," AIChE Journal, Vol. 31, No. 10, 1985, 1605-1613.